ELSEVIER

Biophysical Chemistry 61 (1996) 73–84

Biophysical Chemistry

Attractive adsorbate interaction in biological surface reactions

Håkan Nygren

Department of Anatomy and Cell Biology, University of Göteborg, Medicinaregatan 5, S-413 90 Göteborg, Sweden

Received 23 November 1995; revised 24 January 1996; accepted 13 February 1996

Abstract

Recent studies on ferritin adsorption have revealed strong adsorbate interactions during adsorption (H. Nygren, Biophys. J., 65 (1993) 1508).

In the present study, efforts were made to quantify the attractive lateral adsorbate interaction and to describe the effect of such interactions on the time- and concentration dependence of biological surface reactions.

Attractive forces between ligands increase the time that they are considered neighbours to other ligands. Thus, the inter-ligand interaction effects their distribution and this can be measured experimentally by the pair correlation function $g(r)$.

The attractive lateral interaction was shown to affect the surface adsorption of ferritin, virus particles and bacteria, but played a minor role in the binding of antibodies to surface-immobilised antigen.

Keywords: Surface reaction; Adsorbate interaction; Ferritin adsorption; Virus adsorption; Bacteria adsorption; Attractive interaction

1. Introduction

In 1906, Freundlich [1] suggested an empiric formula describing the adsorption isotherm of organic molecules from water onto surfaces, based on a fractional concentration dependence, $C^{1/P}$.

The mathematical form of the expression is modern in the sense that it is a fractal [2], with an exponent often less than unity. With the advent of Langmuir's firmly established thermodynamic theory of adsorption [3], Freundlich isotherms were interpreted as a sum of several different Langmuir isotherms, i.e. heterogeneity of adsorption energies [4].

In surface catalysis, deviation from Langmuir isotherms is well known [5], and isotherms developed on a linear variation of adsorption energies have been shown to give rate expressions that closely resemble those for a uniform surface [6]. Thus, heterogeneity of the adsorption may not be the only cause of the fractal isotherm.

Deviations from ideal isotherms can also result from adsorbate interactions [7,8]. Surface-phase condensation (self-organisation) owing to an attractive adsorbate interaction almost always results from adsorption of simple molecules onto metal surfaces [5,9].

Attractive adsorbate interactions give autocatalytic reactions, the rate of which can be described by exponential expressions [10].

Recently, the logarithmic time dependence of chemical reactions has been termed "fractal kinetics", which describes autocatalytic reactions at interfaces [11]. Experimental data on protein adsorption at liquid–solid interfaces and antibody binding to surface-immobilised antigen can be described by

0301-4622/96/$15.00 Copyright © 1996 Elsevier Science B.V. All rights reserved.
PII S0301-4622(96)00022-1

fractal time exponents [12–14]. However, in order to describe the entire process of protein adsorption or antibody binding, more than one fractional exponent has to be used, one initial exponent that is greater than unity and a later one that is less than unity [15]. On examining further the adsorption isotherms, it has also been found that more than one exponent is needed to describe the whole adsorption isotherm [16]. This finding is mainly due to the increased sensitivity of modern detection systems, revealing also the initial kinetics of adsorption or the initial phase of an adsorption isotherm. These high-sensitivity measurements show that the initial kinetics is accelerated (t^n; $n > 1$) and the initial phase of the isotherm shows positive cooperativity (C^n; $n > 1$) whereas the later parts of the kinetics show retardation of adsorption (t^n; $n < 1$) and the isotherm at high concentrations is of the Freundlich type (C^n; $n < 1$) far below the point of surface saturation.

At high concentration the amount of adsorbate may even decrease and give hyperbolic isotherms [17]. These isotherms cannot be described by Freundlich or Langmuir isotherms. Theoretical descriptions of these so-called composite isotherms using a linear correction term have been suggested [17].

The aim of the present paper is to demonstrate the importance of attractive interactions in biological surface reactions.

2. Materials and methods

2.1. Transmission electron microscopy (TEM) of virus and protein adsorption

Quartz was used as a substrate for adsorption of virus particles and proteins. Sample supporting grids were made by micromachining of thermally oxidised quartz, as described previously [18]. The substrate was made hydrophobic with hexamethyldisilazane, reacting spontaneously with the surface in a saturated atmosphere at room temperature [16]. The TEM experimental procedure has been described elsewhere for studies of adsorption of phage-λ virus particles [19], ferritin [16], or fibrinogen [20]. Shortly afterwards, the specimens were diluted in phosphate-buffered saline (PBS) and grids were incubated for various periods of time. The grids were rapidly rinsed, stained with uranyl acetate and examined in with Philips 300 electron microscope.

2.1.1. Image analysis

The number of adsorbed particles was counted. The fractal dimensions of the aggregates was analysed by counting the number of adsorbed particles as a function of the distance from a chosen origin. The pair-correlation function was calculated from this data by normalising the number of particles found with an expected number with random distribution over the surface [14].

The energy of interaction was calculated from the size of the deviation of the pair-correlation function from the random distribution [19].

2.2. Light microscopy of bacterial adhesion

Strains of oral streptococci (*Streptococci Sanguis*) were obtained from Dr N. Strömberg, Dept of Cariology, University of Umeå. The bacteria were diluted in PBS and the solution was pumped through a pair of parallel microscopy slides which were glued together leaving a gap of 1 mm. The adsorption of bacteria was monitored with a light microscope, equipped with a video camera. The experimental design has been described in detail by others [21]. The number of adhering cells were counted every 2 s.

2.3. Macroscopic particle aggregation

The mechanism of formation of two-dimensional aggregates was studied in a macroscopic system using paraffin pellets (8 mm diameter) floating on a water surface. The pellets slowly formed fractal aggregates and the process was followed with a time-lapse photographic technique.

2.4. Measurement of protein adsorption with ellipsometry and enzyme-linked immunosorbent assay (ELISA)

Real-time recording of ferritin adsorption was made with comparison ellipsometry at a time resolution of 0.1 s as described previously [22].

The ELISA was performed as a spot test on glass slides as described in detail previously [23]. Fibrino-

gen was adsorbed onto the surface from a PBS solution. The amount of adsorbed fibrinogen was measured with the ELISA. The ELISA assay was calibrated by measuring the surface concentration of fibrinogen using ellipsometry [23]. The effect of adding water-soluble polymers to the fibrinogen solution was measured.

2.5. Binding of radiolabelled antibodies to surface-immobilised antigen

Monoclonal antibodies against the hapten dinitrophenylbenzene (DNP) or against tumour cell antigen (can ag 347625) were radiolabelled with 3H-cyanoborohydride and formaldehyde as described elsewhere [24]. The antibodies were from Prof. M. Steward, London School of Hygiene and Tropical Medicine, and Dr L. Lindholm, University of Göteborg, respectively. Polystyrene microtiter wells (Dynatech) were coated with antigen by adsorption from PBS over night. The hapten was coupled to serum albumin as carrier [24].

Labelled antibodies were incubated in antigen-coated wells over night. The wells were dissolved in xylene. The samples were examined in a scintillation counter. The number of counts per minute were calibrated against reference samples with known antibody concentrations. Results are presented as the mean of two samples [24].

3. Results and discussion

3.1. Adsorption of particles

3.1.1. Phage-λ virus

The kinetics of adsorption of phage-λ virus to a hydrophobic quartz surface is shown in Figs. 1 and 2. The adsorption process is initiated at approximately 10^8 sites per square centimetre, with particles distributed as single entities, pairs or small clusters (Fig. 1(a)).The number of adsorbed virus particles increases slowly with time. A plot of the kinetics of adsorption is shown in Fig. 2. The initial adsorption is found to be rapid, followed by a continuously decreasing rate of adsorption (logistic growth). By extending the time axis up to 10^5 s (Fig. 2(b)), we see that the adsorption process continues slowly through this time period. The kinetics of adsorption from 20 to 10^5 s can be described by a fractal time exponent of $t^{0.15}$ ($R > 0.999$).

The spatial distribution of the particles during adsorption is shown in Fig. 1(b)–(d). Adsorbed particles are found in almost linear clusters with large uncovered areas in between. The fractal dimension of clusters is low after 320 s adsorption time (Fig. 3). Clusters with equally low fractal dimensions are seen during adsorption of paraffin particles at water surfaces [25] and during adsorption of ferritin at liquid–solid interfaces [26].

The concentration dependence of adsorption at 10^5 s adsorption time is shown in Figs. 4 and 5. As can be seen, the number of particles adsorbed at the surface is concentration dependent. Adsorbed particles are distributed as clusters with large uncovered areas in between (Fig. 4).

A plot of the concentration (C) dependence (Fig. 5) shows a linear relation between the number of adsorbed particles (N) and $\log(C)$. The relation can be described by $N = 12.13 + 7.87 \log(C)$ ($R > 0.999$).

Virus adsorption is often regarded as an irreversible process [27]. This assumption is probably not a correct one, since an irreversible reaction would always result in the formation of a monolayer of adsorbed particles at the surface. Instead we see large uncovered areas and a logarithmic concentration dependence of the reaction. This fact is only compatible with the assumption of a reversible adsorption process. However, it is not necessarily reversible upon dilution, but in the presence of new particles arriving at the surface.

The most fruitful description of experimental data may be the pair correlation function of the distribution of particles (Fig. 6). The pair correlation function $g(r) = n(r)/n_0$ where $n(r)$ is the particle density at a distance r from a given particle and n_0 is the mean density of particles. As can be seen, the virus particles show a uniform distribution ($g(r) = 1$) at high surface concentrations, and a more condensed distribution at low surface concentrations. This finding is in accord with similar data on the pair correlation function of adsorbed ferritin [15,17]. The homogeneity of the distribution seen experimentally can thus be quantitated. The probability of finding a particle as a nearest neighbour depends on its mobil-

ity and on the force of interparticular interaction, which can be illustrated by Boltzmann's barometer formula: $N = N_o \exp(-mFd/kT)$, where m is the mass of the particle, F is the interparticle acceleration, and d is distance.

The slope of the plot of $g(r)$ at a coverage of 2.5% can be fitted to an exponential function, $g(r) = 1 + 19.6\exp(-0.698r)$. The found particle distribution within one radius from a chosen particle is then 9.75 times the expected number of particles assuming a random distribution. This relation can be used to calculate the interaction energy [28] as $w(r) = -\ln g(r)$. The interaction energy is thus 2.27 kT at low surface concentration.

3.1.2. Macroscopic two-dimensional particle aggregation

Aggregates, formed spontaneously by floating paraffin particles are shown in Fig. 7(a). The process of aggregation is slow enough to allow studies by

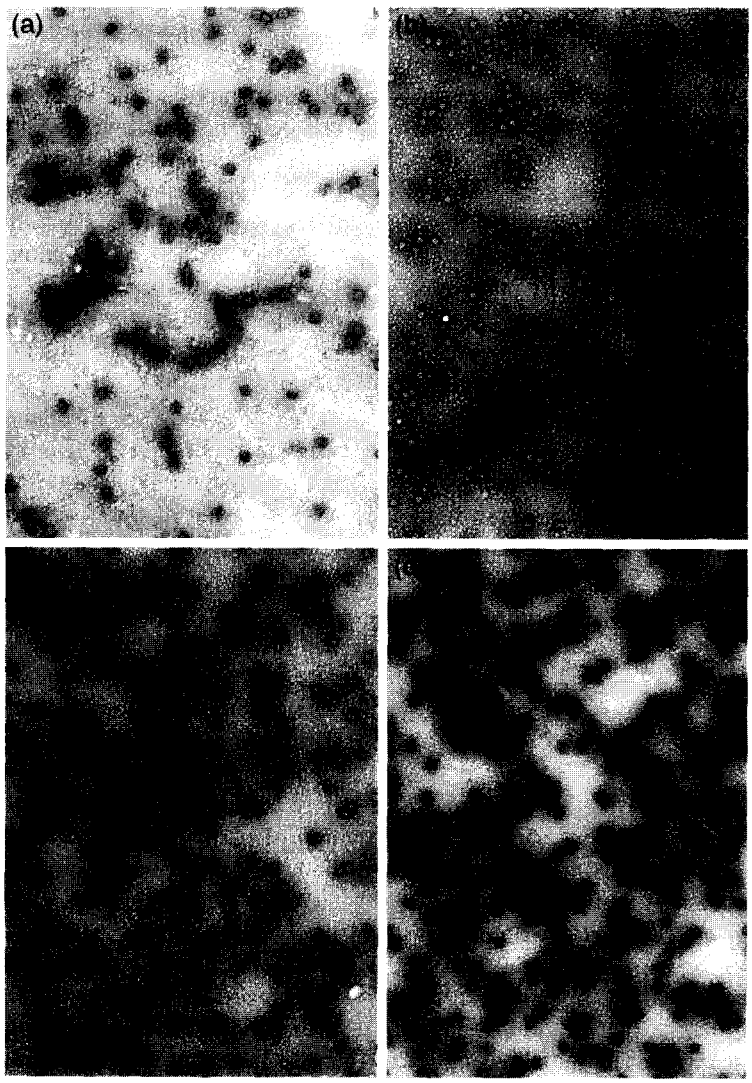

Fig. 1. Electron micrographs of the kinetics of adsorption of phage-λ virus particles onto a methylised silicon surface. The bulk concentration of particles was 6.5×10^{11} per mililitre dissolved in PBS. The adsoption was stopped by rinsing with uranyl acetate (1%) and the grids were blotted dry with filter paper. The diameter of the particles is approximately 50 nm. (a) Adsorption time, 5 s; (b) adsorption time, 20 s; (c) adsorption time, 80 s; (d) adsorption time, 320 s.

simple ocular inspection. Small aggregates are formed by irreversible, diffusion limited aggregation (DLA; sticking probability = 1). The sticking of two approaching particles is influenced by surface forces seen as an accelerating movement of the particles within a distance of approximately one diameter. The morphology of larger aggregates is determined by forces acting between branches of linear aggregates. The resulting, stable clusters are either double rows or dense, round clusters.

The morphology of the aggregates shown in Fig. 7(a) shows that DLA clusters may be polymorphous. The computer-simulated DLA structures with a fractal dimension of 1.67, shown by Witten and Sander [29] are very unlikely to occur in nature, since the forces that makes the particle stick will also be acting between branches within the aggregate.

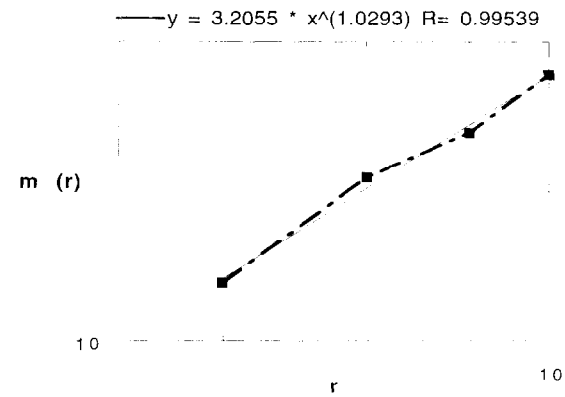

Fig. 3. A plot of the mass distribution of virus particles adsorbed during 320 s from a solution with $C = 6.5 \times 10^{11}$ particles per mililitre. The number of particles found at a distance from a given particle, $M(r)$, $r = 25$ nm, was normalised against the average number of particles n_0. The clusters of virus particles formed at the surface have a low fractal dimension ($d_f = 1.03$).

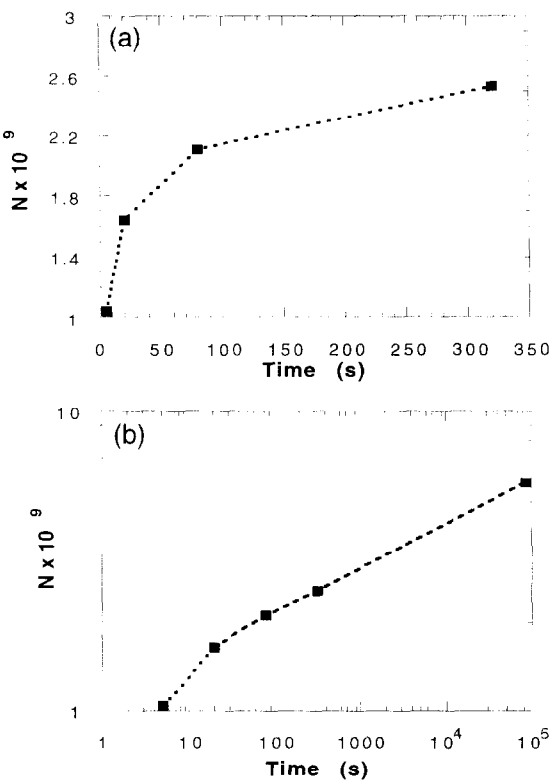

Fig. 2. A plot of the kinetics of virus adsorption shown in Fig. 1. (a) A linear plot of the number of adsorbed particles per square centimeter versus time. (b) A log–log plot extended up to 10^5 s. The surface concentration of adsorbed particles can be fitted to the power law $N = kCt^{0.15}$.

Electron micrographs of aggregates of ferritin, formed during the initial adsorption of the protein onto a hydrophobic surface are shown in Fig. 7(b). The morphology of these aggregates is very similar to that of the aggregates formed by paraffin particles. This is also in accord with computer simulations of the initial adsorption of ferritin, suggesting reversible DLA with conservation of the number of particles present at the surface (restructuring) as the iterated rule behind the morphology of these aggregates [30].

3.1.3. *Str. Sanguis*

The adsorption of *Str. sanguis* from a solution containing 10^{10} cells per mililitre onto a hydrophobic glass surface is shown in Fig. 8. As can be seen, the adsorption of cells is a reversible and discontinuous process for the entire adsorption period. Note that the number of bacteria was counted within the same visual field throughout the experiment and that all cells were counted every 2 s. The observed variation in the number of adsorbed cells is thus a real variation and not due to experimental errors. After an initial lag-phase, the kinetics of adsorption can be described by an exponential function, but may also be considered as linear in this interval (Fig. 8). The results show that adsorption of bacterial cells to a surface is a complex process, very similar in nature to the growth of whole populations [31]. The curve describing the initial kinetics of bacterial adsorption

is equal to the initial part of the logistic growth curve.

The later part of the adsorption process and the pair correlation function of adsorbed cells has been well described by others [21]. The pair correlation function, $g(r)$, was found to be close to a random distribution, suggesting weak intercellular attraction. This finding is in accord with data presented in Fig. 8, showing rapid fluctuations in the number of adsorbed cells, and a low exponential coefficient, giving almost linear kinetics.

The experimental data on bacterial adhesion are, as shown by others, similar to those of particle adsorption [21] and the adsorption data are well fitted to the theory for particle adsorption suggested by Dabros and Van de Ven [32], $N = I[1 - \exp(-\beta_0 t)]/\beta_0$ where I is the flux of particles to the surface and β_0 the residence time.

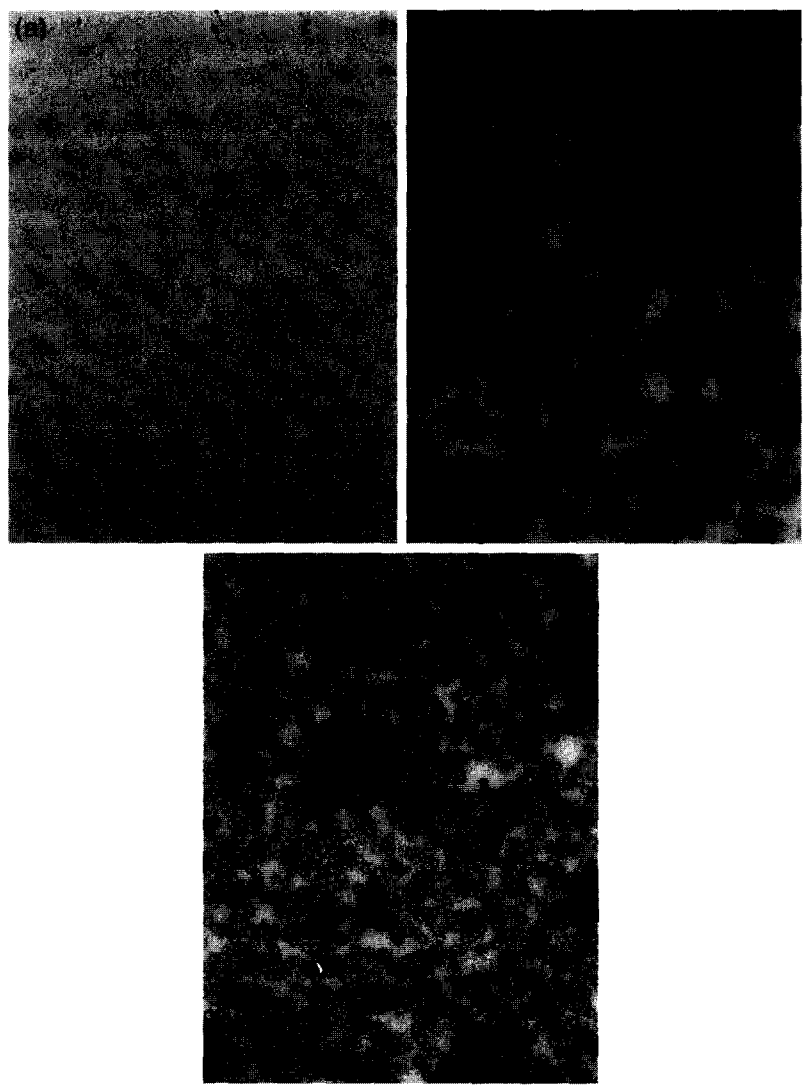

Fig. 4. Electron micrographs of the adsorption of phage-λ virus particles onto a methylised silicon surface. The adsorption time was 24 h. The bulk concentration of particles was 6.5×10^{11} per mililitre, diluted 1:1, 1:5 and 1:25 in PBS. The adsoption was stopped by rinsing with uranyl acetate (1%) and the grids were blotted dry with filter paper. The diameter of the particles is approximately 50 nm. (a) C = 1:25; (b) C = 1:5; (c) C = 1:1.

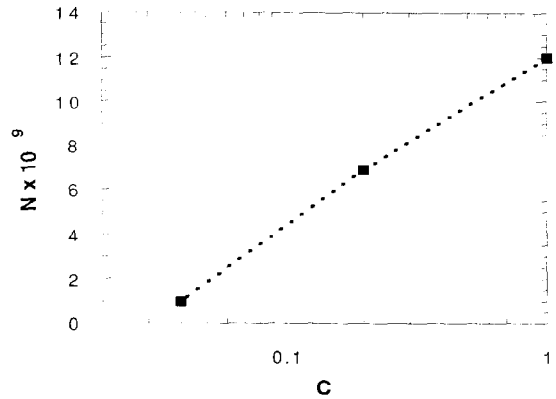

Fig. 5. A plot of the adsorption of virus particles versus concentration (data from Fig. 4. $C = 1$ corresponds to a bulk concentration of particles of 6.5×10^{11} per mililitre. The adsorption isotherm can be described by the relation $N = 12.13 + 7.87 \log (C)$ ($R > 0.999$).

3.2. Adsorption of polymers and proteins

3.2.1. The kinetics of ferritin adsorption

The kinetics of ferritin adsorption onto a hydrophobic quartz surface, measured with comparison

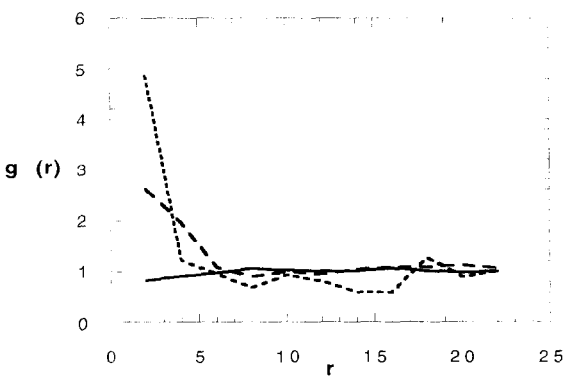

Fig. 6. The pair correlation function $g(r)$ of adsorbed virus particles at different surface concentrations. $\Theta = 0.3$ (solid line); $\Theta = 0.18$ (broken line); $\Theta = 0.025$ (dotted line). $\Theta = N/N_{max}$, where $N_{max} = 4 \times 10^{10}$ particles per square centimeter.

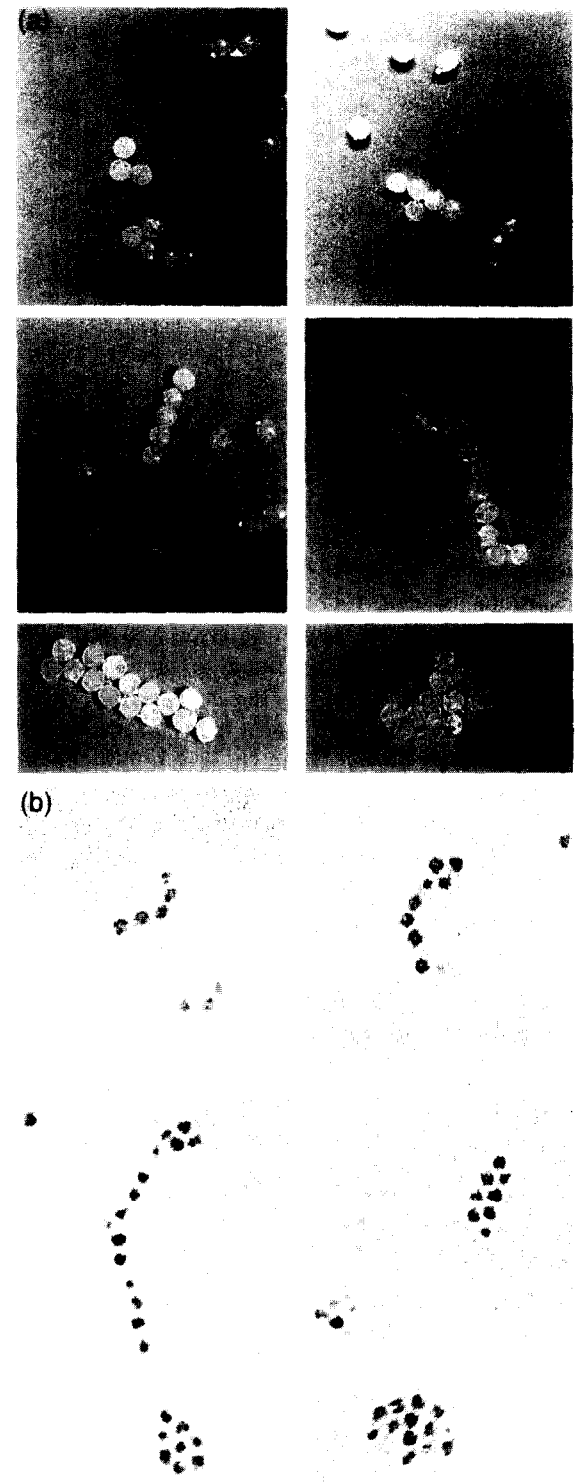

Fig. 7. Photographs and electron micrographs of clusters formed during the intitial formation of two-dimensional aggregates at liquid interfaces. (a) Photographs of restructured DLA-clusters of paraffin particles (8 mm diameter) formed during free floating at an air–liquid interface. (b) Electron micrographs of clusters of ferritin particles formed during adsorption on a hydrophobic surface.

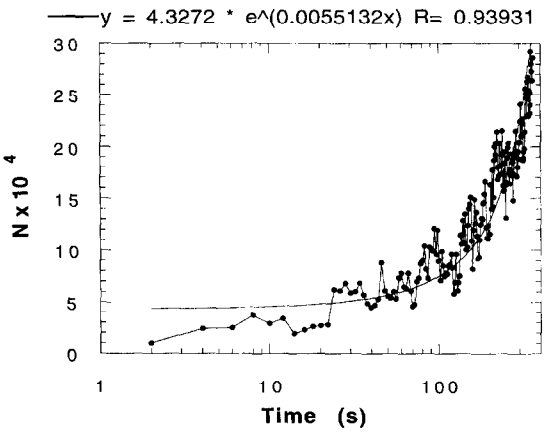

Fig. 8. The initial adsorption of a bacterial strain (*Strept. sanguis*) to a glass surface as observed by light microscopy, together with a best-fit exponential function. All adsorbed cells were counted every 2 s.

ellipsometry, is shown in Fig. 9. A rapid initial adsorption is seen, followed by a continuously decreasing rate of adsorption (logistic growth). The initial adsorption can be fitted to an exponential function as seen in a log–linear plot (Fig. 9(b)). However, there are two linear parts of the curve, with different slopes. Thus, it is not possible to define a single forward rate exponent.

An exponential fit of the initial part of the kinetic curve of ferritin adsorption from different bulk concentrations is shown in Table 1. As can be seen, the value of the exponents varies for different bulk

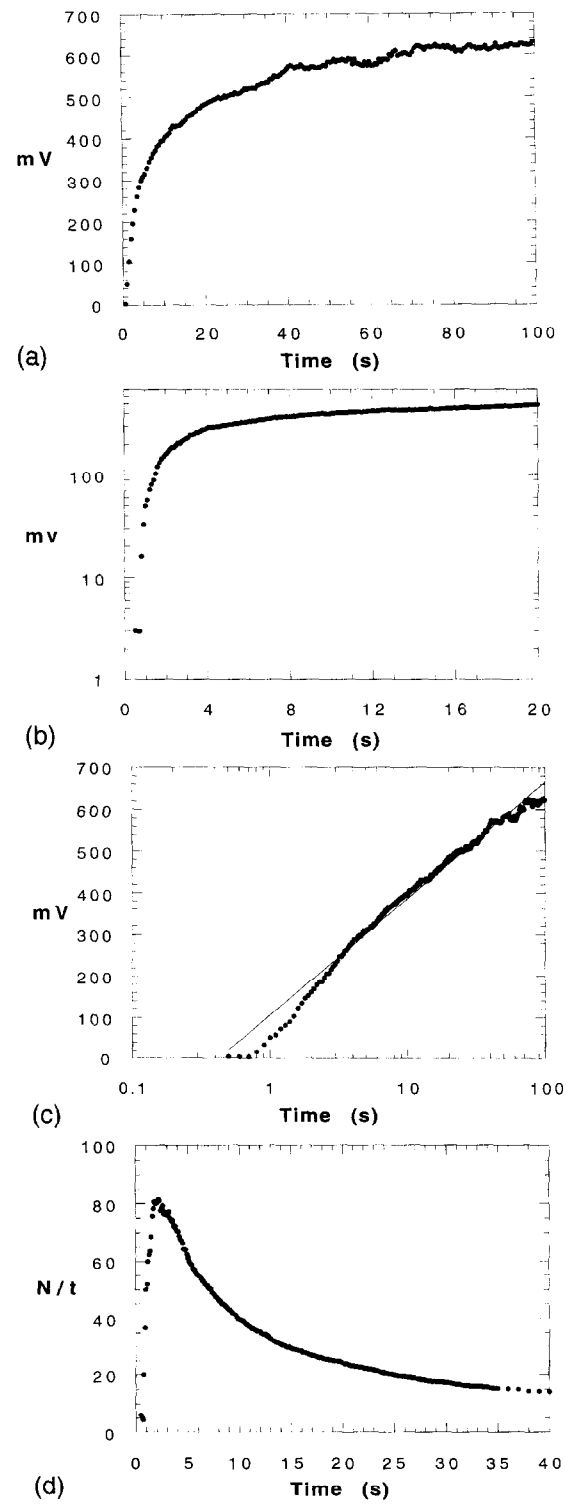

Fig. 9. Ferritin adsorption from phosphate-buffered saline onto a hydrophobic quartz surface measured with comparison ellipsometry at a time resolution of 0.1 s. The light intensity passing through the instrument (mV) is directly proportional to the thickness of the adsorbed layer, and can be used without further calculations as a measured value of the surface concentration of bound ferritin (N). For further details see Ref. [25]. (a) A linear plot of the kinetics of ferritin adsorption from a bulk concentration of 1 g l^{-1}. (b) A log–linear plot of data from Fig. 11(a) showing that the initial adsorption can be fitted to an exponential equation. Note that there are at least two linear parts with different slopes. (c) A log–linear plot of data from Fig. 11(a) showing that the later part of the adsorption process is linear with log (t). (d) A probabilistic plot of ferritin adsorption. The surface concentration of adsorbed feerritin is regarded as the number of succesful attempts to bind, and It represents the total number of attempts to bind. N/t plotted versus t, then represents a probabilistic plot of the binding reaction.

concentrations of the protein. This finding is an argument for including concentration in the exponent.

The finding that the rate exponent may decrease with increasing concentration indicates that the adsorption process is a complex one. This complexity can be included in a theoretical model describing the process, by assuming a concentration-dependent desorption taking place simultaneously with the adsorption.

The slower part of the adsorption is linear to log (t) as seen in Fig. 9(c).

A probabilistic plot of the ellipsometry data is shown in Fig. 9(d). As can be seen, the probability of adsorption (N/It) increases initially with time (i.e. It), reaches a maximum and then decreases.

3.2.2. *Isotherm of fibrinogen adsorption*

The concentration dependence of fibrinogen adsorption onto a hydrophilic glass surface is shown in Fig. 10. The surface concentration of adsorbed fibrinogen was measured with a calibrated ELISA after an adsorption time of 72 h.

The initial adsorption is strongly concentration dependent (Fig. 10(a)). At higher bulk concentrations, a weaker concentration dependence of adsorption is seen.

A probabilistic plot of data is shown in Fig. 10(b). The amount of bound fibrinogen is normalised to the bulk concentration, i.e. kCt. The bound:free ratio is plotted versus the surface concentration of bound fibrinogen. This is the well known Scatchard plot [33] that can be given a probabilistic interpretation.

As can be seen, the probability of adsorption at first increases with increasing surface concentration of bound fibrinogen. This phenomenon is often referred to as positive cooperativity [34]. The probability of adsorption then decreases with increasing surface concentration of bound fibrinogen.

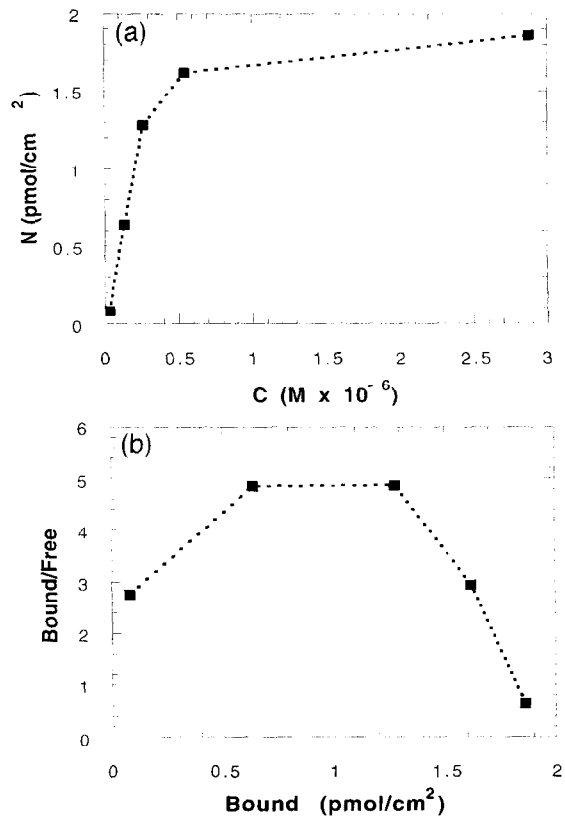

Fig. 10. Isotherms of fibrinogen adsorption, measured with a calibrated ELISA. (a) A linear plot of the isotherm of adsorption onto a hydrophilic glass surface after 72 h adsorption time at room temperature. (b) A probabilistic plot, according to Scatchard, of data shown in Fig. 11(a).

Table 1
Forward rate exponents of ferritin adsorption to a hydrophobic surface as a function of bulk concentration of ferritin (best fit to data)

Concentration(g l^{-1})	Rate equation [a]
10	$N = 17.5 \times 2^{1.3t}$
1	$N = 1.09 \times 2^{1.9t}$
0.1	$N = 4.62 \times 2^{0.76t}$
0.01	$N = 7.27 \times 2^{0.12t}$

[a] $N = kCt\exp(at)$.

An electron micrograph of the spatial distribution of adsorbed fibrinogen is shown in Fig. 11. Orderly arranged molecules of adsorbed fibrinogen are seen at surface concentrations showing positive cooperativity in the Scatchard plot. Molecules contained in orderly arranged layers are not expected to be mobile in accordance with the Boltzmann barometer formula. Measurements of surface diffusion of proteins show the expected low mobility of fibrinogen at surfaces [35].

An initial exponential phase of protein adsorption isotherms, prior to the logarithmic phase was first described by MacRitchie [36] who realised that the

fitting of adsorption data to Langmuir isotherms may be only apparent. This notion was based on the found irreversibility of adsorption upon dilution.

A breakthrough in the irreversibility aspect was made by Brash and co-workers [37,38], who showed desorption of labelled protein in the presence of bulk protein. Data on protein desorption according to first order rate kinetics has also been shown by others [39]. Brash and Samak suggested an empirical model for balanced protein adsorption based on the term, $A[1 - \exp(-\beta t)]$ where A is the exchangeable fraction of protein.

The argument for the model was an experimental finding that the initial part of the binding curve exhibited an exponential form, suggesting first order kinetics [37].

3.3. Antibody binding to surface-immobilised antigen

Isotherms of binding of two monoclonal antibodies with different affinity for a hapten, dinitrophenylbenzene, is shown in Fig. 12(a). At low bulk concentration, no difference can be seen between the isotherms. At high bulk concentrations, the high-affinity antibody shows a higher surface concentration. A probabilistic plot of N/C versus C (Fig. 12(b)), shows a positive cooperativity of binding for both antibodies at low bulk concentrations. A higher probability of binding of the high affinity antibody is also seen at all concentrations. The potential of antibody binding is shown in Table 2. At low bulk concentration, the potential is approximately 10 kT. At higher concentration, an inter-ligand interaction component increases the potential to approximately 10.7 kT. At higher concentrations, the potential decreases back to approximately 9.6 kT.

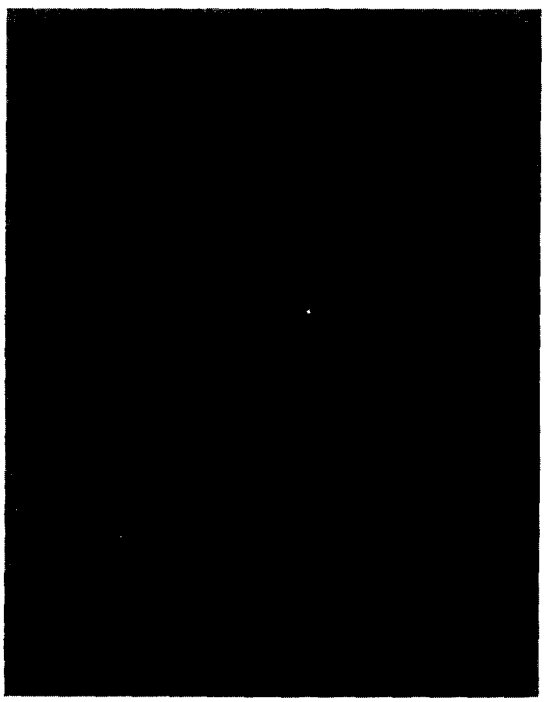

Fig. 11. Electron micrograph of fibrinogen adsorbed onto a hydrophilic quartz grid for 24 h at a bulk concentration of 10 mg l^{-1}.

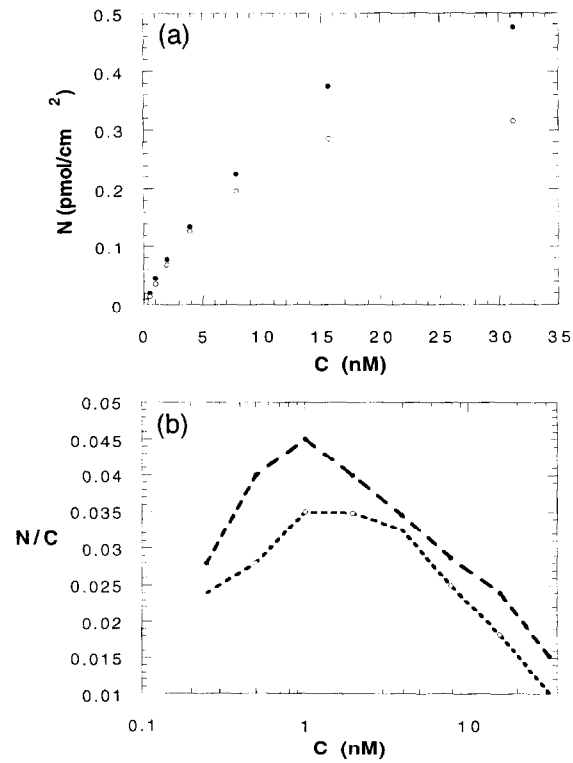

Fig. 12. Binding isotherms of radiolabelled monoclonal antibodies to surface immobilised hapten. (a) A linear plot of the binding isotherms of two antibodies against the same hapten, DNP. The antibodies bind with different affinity to the free hapten in solution, $-K_a = 4.1 \times 10^7$ M^{-1} and $-K_a = 0.35 \times 10^6$ M^{-1}. The difference in affinity is seen as a change in the amount of bound antibodies and not as a shift along the concentration axis. (b) A probabilistic plot of N/C versus C, showing that the probability of binding is higher for the high affinity antibody.

Table 2
The apparent binding potential of antibodies to surface-immobilised hapten

$\Theta \times 10^{-2}$(s)	$\Theta v \times 10^{-6}$	$\log \Theta s / \Theta v$
4.6	3.1	9.6
3.75	1.5	10.1
2.24	0.78	10.3
1.35	0.39	10.5
0.78	0.2	10.6
0.45	0.1	10.7
0.2	0.05	10.6
0.07	0.025	10.2

The cooperativity is thus due to an intermolecular interaction of only 1 kkT, which may explain the close fit of the antibody binding isotherm with classical Langmuir–Scatchard formalism.

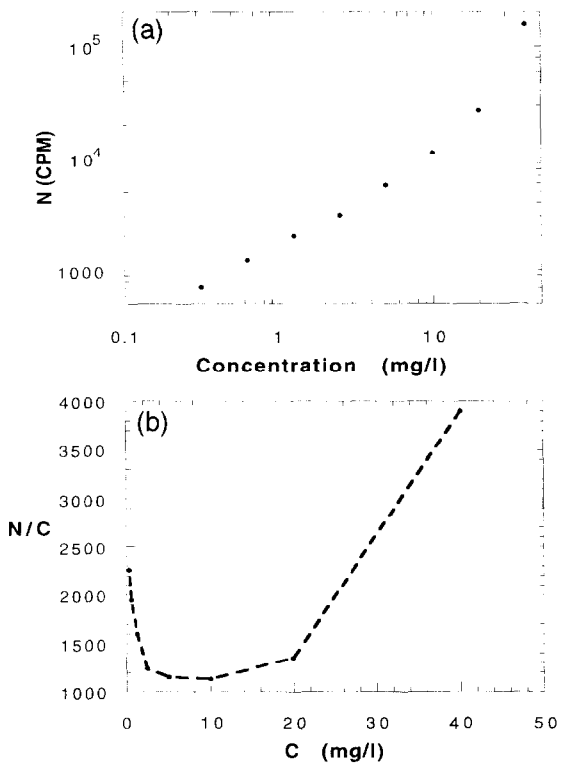

Fig. 13. Binding isotherms of radiolabelled monoclonal antibodies to surface-immobilised tumour antigen. The binding isotherm of an anti-tumour antibody to surface-immobilised tumour antigen. The initial part of the isotherm can be fitted to a Freundlich isotherm with a power law of $C^{0.74}$. The isotherm then bends upwards at a bulk concentration of 10 mg l^{-1}. Above this value, the adsorption isotherm is exponential with respect to C.

Isotherms of binding of a monoclonal antibody against a tumour antigen is shown in Fig. 13. As can be seen, the initial binding can be fitted to a Freundlich isotherm, with a slope of $C^{0.74}$. The curve then bends upward at higher concentrations.

This finding indicates that binding and desorption occurs simultaneously also at low surface concentrations of antibodies, and that positive cooperativity i.e. the upward bend at a bulk concentration of antibodies of 5–10 mg l^{-1}, is only seen in above a critical surface concentration, allowing an ab–ab interaction to occur.

Studies of the binding of antibodies to surface-immobilised antigen with in-situ ellipsometry at a time resolution of 0.5 s has shown that the initial phase of binding can be fitted to an exponential function, before the binding curve becomes logarithmic [40]. The autocatalytic acceleration of antigen–antibody reactions at interfaces can be described by the term [40], $N = aIt[1 - \exp(-\alpha N)]$ where a is the probability of monomolecular binding and α relates to the probability of a favourable interaction between bound and arriving molecules. In the present study we may define the stage of antibody binding preceding the exponential phase. The onset of the exponential phase may also be sensitive to the density of binding sites at the surface.

References

[1] H. Freundlich, Z. Phys. Chem., 57 (1906) 385–396.
[2] B.B. Mandelbrot, The fractal geometry of nature, W.H. Freeman and Co, New York, 1977.
[3] I. Langmuir, J. Am. Chem. Soc., 39 (1917) 1848–1854.
[4] J. Shaw, Introduction to Colloid and Surface Chemistry, Butterworths, London, 1980.
[5] J.A. Benziger and G.R. Schoofs, J. Phys. Chem., 88 (1984) 4439–4442.
[6] M. Boudart, in H. Eyring (Ed.), Physical Chemistry. An Advanced Treatise, Vol. VII, Academic Press, New York, 1975.
[7] K.J. Laidler, in P.H. Emmet (Ed.), Catalysis, Vol I, Reinhold, New York, 1956.
[8] T.L. Hill, An Introduction to Statistical Thermodynamics, Addison-Wesley, Reading, MA, 1960.
[9] G.A. Samorjai and H.H. Farrell, Adv. Chem. Phys., 20 (1971) 215–222.
[10] R.J. Madix, in D.A. King and D.P. Woodruff (Eds.), The Chemical Physics of Solid Surfaces and Heterogeneous Catalysis, Vol 4, Fundamental Studies of Heterogeneous Catalysis Elsevier, Amsterdam, 1982, Chapter 1, pp. 1–25.

[11] R. Kopelman, Science, 241 (1988) 1620–1623.
[12] P.A. Cuypers, G.M. Willems, J.M.M. Kop, J.W. Corsel, M.P. Jansen and W.T. Hermens, Proteins at Interfaces. Physicochemical and Biochemical Studies. ACS Symp. Ser. 343, American Chemical Society, Washington, 1987, pp. 208–214.
[13] M. Werthen, M. Stenberg and H. Nygren, Progr. Colloid Polym. Sci., 82 (1990) 349–352.
[14] H. Nygren, Biophys. J., 65 (1993) 1508–1512.
[15] H. Nygren, H. Arwin and S. Welin, Colloids Surfaces A: Physicochem. Eng. Aspects, 76 (1993) 87–90.
[16] H. Nygren and M. Stenberg, Biophys. Chem., 38 (1990) 77–86.
[17] J.J. Kipling, Adsorption from Solutions of Non-electrolytes, Academic Press, New York, 1966.
[18] M. Stenberg, S. Stemme and H. Nygren, Stain. Technol., 62 (1987) 231–234.
[19] M. Stenberg and H. Nygren, Phys. Rev. Lett., 59 (1987) 1164–1167.
[20] H. Nygren and M. Stenberg, J. Biomed. Mater. Res., 22 (1988) 1–11.
[21] J. Sjollema, Thesis, University of Groningen, 1992.
[22] H. Nygren, Colloids Surfaces B: Biointerfaces, 4 (1995) 243–250.
[23] C. Karlsson, A. Karlsson, M. Stenberg and H. Nygren, Colloid Polym. Sci., 270 (1992) 377–383.
[24] M. Werthen and H. Nygren, Biochim. Biophys. Acta, 1162 (1993) 326–330.
[25] A. Hurd and D. Schaefer, Phys. Rev. Lett., 54 (1985) 1943–1946.
[26] H. Nygren and M. Stenberg, Progr. Colloid Polym. Sci., 82 (1990) 15–18.
[27] C.P. Gerba, Adv. Appl. Microbiol., 30 (1984) 133–144.
[28] R.S. Berry, S.A. Rice and J. Ross, Physical Chemistry, J. Wiley and Sons, New York, 1980, pp. 433.
[29] T.A. Witten and L.M. Sander, Phys. Rev. Lett., 47 (1981) 1400–1405.
[30] M. Stenberg and H. Nygren, Progr. Colloid Polymer Sci., (1990) 1–6.
[31] R.M. May, Nature, 261 (1976) 459–463.
[32] T. Dabros and T.G.M. Van de Ven, J. Colloid Interface Sci., 89 (1982) 232–243.
[33] G. Scatchard, Ann. N.Y. Acad. Sci., 51 (1949) 660–663.
[34] T.E. Creighton, Proteins, W.H. Freeman and Co, New York, 1984, Chapter 8, p. 336.
[35] H. Nygren, S. Alaeddine, I. Lundström and K.-E. Magnusson, Biophys. Chem., 49 (1994) 263–269.
[36] F. MacRitchie, J. Colloid Interface Sci., 38 (1972) 484–490.
[37] J.L. Brash and Q.M. Samak, J. Colloid Interface Sci., 65 (1978) 495–503.
[38] B.M.C. Chan and J.L. Brash, J. Colloid Interface Sci., 82 (1981) 217–222.
[39] M.E. Soderquist and A.G. Walton, J. Colloid Interface Sci., 75 (1980) 386–394.
[40] H. Nygren, Biophys. Chem., 52 (1994) 45–49.